RESEARCH ARTICLE | JANUARY 24 2019

# Quasi-steady-state photoconductance bulk lifetime measurements on silicon ingots with deeper photogeneration

Mohsen Goodarzi ; Ronald Sinton; Daniel Macdonald



*AIP Advances* 9, 015128 (2019)
https://doi.org/10.1063/1.5086378

# Quasi-steady-state photoconductance bulk lifetime measurements on silicon ingots with deeper photogeneration

Cite as: AIP Advances 9, 015128 (2019); doi: 10.1063/1.5086378
Submitted: 20 December 2018 • Accepted: 10 January 2019 •
Published Online: 24 January 2019

View Online Export Citation CrossMark

Mohsen Goodarzi,[1] Ronald Sinton,[2,a)] and Daniel Macdonald[1]

## AFFILIATIONS

[1]Research School of Engineering, The Australian National University, Canberra ACT 2601, Australia
[2]Sinton Instruments Inc., Boulder, Colorado 80301, USA

[a)]http://www.sintoninstruments.com

## ABSTRACT

Quasi-steady-state photoconductance measurements on silicon ingots and blocks with different photo-generation profiles are simulated in this work. The results show that deeper generation profiles, achieved by using a long-pass optical filter with a longer cut-off wavelength, can reduce the impact of the high surface recombination velocity of the ingot surface. This results in higher measured effective lifetimes and reduces the reliance on transfer functions to convert the measured lifetimes into bulk lifetimes. However, there exists a trade-off between generating carriers further from the surface to reduce surface recombination and ensuring that the generated carriers are within the sensitivity range of the photoconductance sensing coil. The simulations are compared with experimental results measured on a monocrystalline silicon block using both quasi-steady-state and transient photoconductance decay, as the transient method is relatively less prone to the impact of surface recombination, and provides a lower bound on the bulk lifetime. The results confirm an increased accuracy in bulk lifetimes extracted from quasi-steady-state measurements when measured using deeper photo-generation profiles.





## I. INTRODUCTION

As a very well established method for the measurement of carrier lifetimes on silicon wafers, the quasi-steady-state photoconductance (QSSPC) method[1] has also been recently applied to ingot and block lifetime measurements, and the characterization of crystal defects and impurities within them.[2,3] This application can provide more immediate feedback on crystal growth quality through specific knowledge about the impurities and crystal defects in the ingots and blocks. This may lead to making more reliable decisions for cropping ingots and blocks for wafering purposes. It may also be possible to sort the wafers at the start of processing and tune the cell process for different quality wafers coming from the different sections of the block.[4] Microwave-detected photoconductance decay mapping has also been the most commonly used method for monitoring carrier lifetimes on silicon ingots.[5] More recently, other characterization methods capable of providing such information at the ingot level have been developed, such as the QSSPC method,[6] which is used in this work, and Photoluminescence (PL)-based methods for ingot characterization.[7,8]

One of the advantages of ingot and block characterization is that there is no need for any surface treatments prior to the lifetime measurements. However, this introduces the difficulty of the presence of a high surface recombination velocity (SRV). Previous studies have investigated the effect of a high SRV and sample thickness on the excess carrier lifetime in silicon wafers and blocks using a dynamic photoluminescence approach.[9,10] It has also been shown that a high SRV can introduce large deviations between the measured and actual bulk lifetime.[4,6,11] In practice, the measured (effective) lifetime, $\tau_{effective}$ is limited by surface recombination and Shockley–Read–Hall (SRH) recombination centres in the bulk, in addition to intrinsic recombination due to Auger and radiative recombination:[12]

$$\frac{1}{\tau_{effective}} = \frac{1}{\tau_{Auger}} + \frac{1}{\tau_{rad}} + \frac{1}{\tau_{SRH-bulk}} + \frac{1}{\tau_{surface}}$$

or

$$\frac{1}{\tau_{effective}} = \frac{1}{\tau_{bulk}} + \frac{1}{\tau_{surface}} \quad (1)$$

It is important to eliminate the surface recombination component when reporting the bulk lifetime. To address this issue in QSSPC measurements, Bowden and Sinton[4] introduced a transfer function which estimates the bulk lifetime from the measured effective lifetime by simulating the effect of a high SRV.

It has been shown that shifting the excess carrier profile peak deeper into the sample, by using deeper photogeneration, will increase the accuracy of the lifetime reported in the transient photoconductance method.[13] Schuler *et al.*[14] demonstrated the improved accuracy of lifetime measurements by using a deeper generation profile in MDP (Microwave Detected PhotoConductance) as a method with steady-state photogeneration, in comparison with μPCD (microwave detected PhotoConductance Decay) as a method with transient photogeneration, on thick silicon samples. Johnston *et al.*[5] compared PL images of the brick surfaces to minority-carrier lifetimes measured by resonant-coupled photoconductive decay (RCPCD) demonstrating the advantage of the long penetration depth of long-wavelength light in the range of 1150 nm. Mitchell *et al.*[8,15] used the intensity ratio of two PL images taken with two different filters in front of the camera to determine the bulk lifetime. More recently, Chung *et al.* demonstrated a PLIR method using two different excitation wavelengths of 915 and 1064 nm to generate different carrier profiles with deep generation.[16]

In this work, a model for simulating QSSPC lifetime measurements in silicon blocks (as explained in Ref. 2) is used, with an emphasis on studying the impact of deeper photogeneration profiles on the accuracy of the QSSPC lifetime measurements. The deeper generation profiles are generated using longer cut-off wavelength long-pass filters in front of the flash. The simulation results are confirmed by measurement on a Cz p-type monocrystalline silicon block using a "BCT-400" measurement system from Sinton Instruments. The results are also compared to lifetime measurements in transient mode as a method which does not require calculation of the generation rate, or the application of transfer functions, and which provides a lower bound on the bulk lifetime.

## II. SIMULATIONS

The model and simulation tool explained in detail in Ref. 2 is used here to study the effect of deeper photo-generation profiles on the measured lifetime in the QSSPC method. As mentioned in Ref. 2, a significant challenge in applying the QSSPC technique to a block is its large depth (thickness) which can be considered as infinite in comparison to the minority carrier diffusion length. Hence, the excess carrier density, $\Delta n$, profile in a block is never uniform.[2,4] A weighted average excess carrier density, $\Delta n_{avg}$, was introduced by Bowden and Sinton[4] to address these problems:

$$\Delta n_{avg} = \frac{\int_0^\infty \Delta n^2 dx}{\int_0^\infty \Delta n\, dx} \quad (2)$$

### A. Optical specifications

Figure. 1 illustrates the spectrum of the X5dR Q xenon flash along with the EQE of the reference cell typically used in the BCT-400 tool, and transmission functions for the four filters used and simulated in this work. The filters are two IR-Pass Schott glass 850 and 1000 nm filters (RG850 and RG1000), of which the RG1000 is the standard filter currently used with the BCT-400 tool, as well as two high-performance OD 4 long-pass filters from Edmund Optics with sharp cut-off wavelengths at 1050 nm (EO1050) and 1100 nm (EO1100) respectively. The two EO filters have sharper edges and greater transmission at longer wavelengths in comparison with the RG850 and RG1000. This will generate excess carrier densities deeper in the bulk as the photons with shallower absorption coefficients are removed by the filters. However, it will also tend to decrease the maximum injection level created in the sample due to the lower total photon flux.[13]

The advantage of deeper generation is that the $\Delta n$ peak will be more distant from the surface, and fewer carriers will diffuse to the surface to recombine. However, in the QSS mode of measurement, there will be constraints imposed by the tool depth sensitivity and the reference cell EQE on how deep the generation profile can be in practice. As shown in Equation (3), accurate determination of the cumulative photogenerated carriers across the sample is crucial to calculate the effective lifetime $\tau_{effective}$.

$$\tau_{effective} = \frac{\Delta n\, W}{G_{cum}} \quad (3)$$

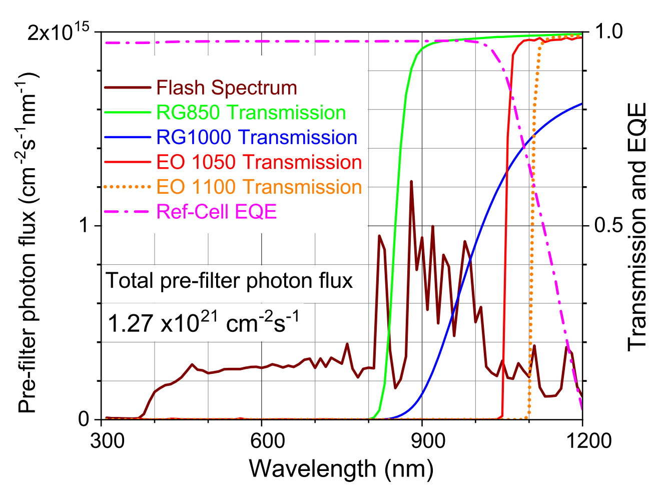


**FIG. 1**. Xenon flash spectrum, reference cell EQE and measured filter transmission functions.

A reference cell is used to determine the cumulative generation rate $G_{cum}$ during the measurement in the QSS mode. As can be seen in FIG. 1, a longer cut-off wavelength will push the generation spectrum closer to the part of the spectrum in which the reference cell EQE exhibits a sharply decreasing tail. This will add uncertainty to the determination of the cumulative photogenerated carriers which consequently results in uncertainty in the lifetime calculation. FIG. 1 shows the severity of this uncertainty for the EO1100 filter, which makes the $G_{cum}$ determination quite unreliable. Hence, the EO1100 is not considered a suitable choice to improve the accuracy of lifetime measurements in the QSS mode. This conclusion will be supported again in section C below.

As Swirhun *et al.*[3] showed previously, the RG1000 performs significantly better than the RG850. In this work, the RG850 is only used in simulation to confirm the results in Ref. 3 and not included in the experimental results here, where we compare only RG1000 and EO1050 to select the best filter for the QSS measurement.

### B. Generation and carrier densities profiles

FIG. 2 (a) shows the photo-generation profiles required to generate an average excess carrier density of $\Delta n_{avg}$ = $10^{15}$ cm$^{-3}$ in a p-type thick sample with an SRV = $10^{6}$ cms$^{-1}$ for the unpassivated surface. The corresponding excess carrier density profiles for the three filters are illustrated in FIG. 2 (b). The carrier profiles become broader with higher and deeper peaks as the cut-off wavelength is increased. The reason for the higher peaks for deeper generation is that the coil sensitivity decays with depth, and the carriers closer to the surface have a significantly higher impact on $\Delta n_{avg}$ as discussed in Ref. 4. Therefore, a higher initial pre-filter photon flux is needed for the filter with longer cut-off wavelength to generate the same average injection level ($\Delta n_{avg}$ = $10^{15}$ cm$^{-3}$).

Practically, this reduces the maximum injection levels that can be reached when the EO1050 is used. However, this is not a practical disadvantage in ingot and block measurements, as high injection measurements, such as required for $J_0$ measurements on wafers, are not performed on ingots.

The QSSPC lifetime measurements are simulated using the simulation tool introduced in Ref. 2 for various bulk lifetimes in a p-type silicon block with the three filters. The effective lifetimes are expected to be equal to the input bulk lifetime ($\tau_{effective} = \tau_{bulk}$) when SRV = 0.

As illustrated in FIG. 3, the effective lifetimes simulated with the EO1050 filter have a smaller deviation from the bulk lifetimes amongst the three filters. In contrast, the RG850 with the shallowest generation profile, reports the lowest effective lifetime, as more generated carriers diffuse and recombine at the surface before recombining in the bulk. For bulk lifetimes lower than 30μs, the EO1050 and RG1000 filters are relatively close in performance. However, the advantage of deeper generation profiles appears at a bulk lifetime of around 50μs, at which the standard RG1000 filter demonstrates more deviation in the effective lifetime in comparison with EO1050. This deviation increases for longer bulk lifetimes for all filters because the effect of the high SRV, particularly for the RG filters, becomes more significant as the bulk diffusion length increases.

### C. Optical constant

The reference cell in the BCT-400 tool with the illustrated EQE in FIG. 1 is used to measure the light incident on the sample. This is then used to calculate the cumulative photogeneration in the sample during each measurement. Due to the reference cell EQE, as well as reflection from the unpassivated sample surface, there is a discrepancy between the incident light measured by the reference cell and the photogeneration in the sample.



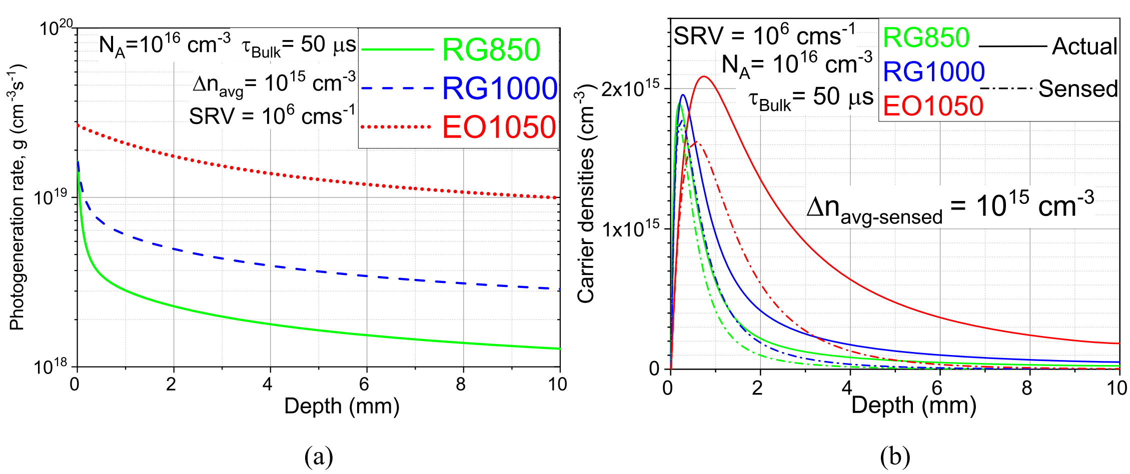


**FIG. 2**. a) Typical generation profiles for 3 filters to generate $\Delta n_{avg}$ = $10^{15}$cm$^{-3}$, and b) Excess carrier density profiles at $\Delta n_{avg}$ = $10^{15}$cm$^{-3}$ under steady-state conditions, as functions of sample depth for the three filters.

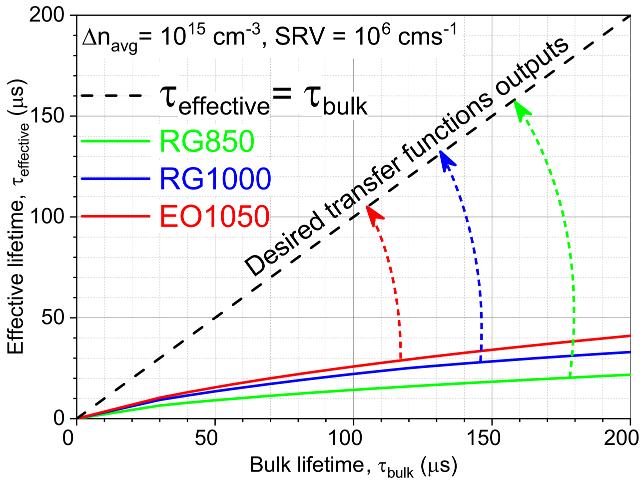


**FIG. 3**. Simulated effective lifetimes as functions of bulk lifetime for three filters (symbol-line). The dashed line indicates equality between the effective lifetime and the bulk lifetime.

An optical constant is therefore required in QSSPC measurements to account for this, and is defined as follows:

$$\textit{Optical constant} = \frac{\textit{Total absorption in the sample}}{\textit{Total absorption in the reference cell}} \quad (4)$$

The assumed depth of absorption in the sample is important in determining the optical constant, particularly for the filters with longer cut-off wavelengths due to their larger proportion of photons with low absorption coefficients. We aim to choose a depth that accounts for all photons absorbed in the sensed region but does not include photons absorbed far below the sensed depth of the sample. The calculated optical constants for each filter are shown in FIG. 4 as a function of depth. Note that 156mm corresponds to the full thickness of a standard '6 inch' rectangular silicon block.

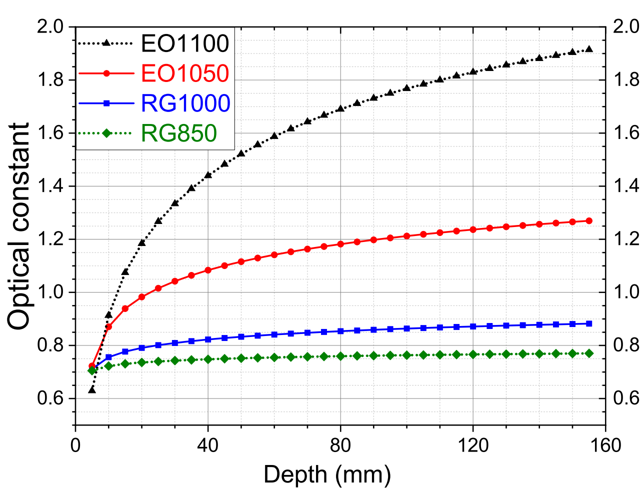


**FIG. 4**. Optical constants for the four filters as a function of depth for a sample with an unpassivated as-cut surface.

FIG. 4 shows an almost flat optical constant as a function of depth for RG850, while there is a gradual change for the RG1000 filter for depths beyond 5 mm, as expected from their shallow generation profiles. A similar trend is observed for EO1050 for depths deeper than 40 mm. However, due to the deeper generation profile of EO1100 and the low EQE of the reference cell in that spectral range, the EO1100 optical constant changes with a larger slope in the depth range up to 150 mm. In principle, this could result in measured effective lifetimes that are less accurate, due to a higher sensitivity to the choice of the optical factor. Therefore, there exists a trade-off between reducing the impact of the high SRV, and the impact of uncertain optical constants. Due to uncertainty in the reference cell EQE in the EO1100 filtered spectrum, the determined cumulative photogeneration is quite unreliable. We, therefore, conclude that the EO1100 filter is not a suitable choice for improved QSS lifetime measurements.

There are several factors to consider when selecting a suitable depth for the optical constant calculation in lifetime measurements, to ensure that the results are not overly affected by generation and recombination beyond that depth. The first is the tool sensitivity depth and its decay constant, which for the Sinton BCT-400 that is used in this work is about 2.5 mm, as discussed in detail in Ref. 3. Minority carrier diffusion into and out of the tool sensitivity range makes the carrier diffusion length another important factor that can affect the results. As the QSS conditions are generally only valid for lifetimes below 200 μs, the maximum expected carrier diffusion lengths in our work is less than 1 mm. Moreover, the rate at which the optical constant value changes as a function of depth can also influence the results, as discussed above.

Considering the above factors, a depth of 10 mm was chosen in this work to calculate the optical constant values for the three filters, as any generation and recombination beyond that depth will certainly not have any effect on the measurement results in this work.

## III. EXPERIMENTAL RESULTS AND DISCUSSION

The QSSPC measurements on a Cz block were performed with a BCT- 400 measurement system from Sinton Instruments in QSS mode with an RG1000 filter and the EO 1050 filters. The sample was a rectangular block cut from a standard industrial Cz p-type monocrystalline silicon ingot, with a square base of 156×156 mm and a height of 320 mm. Initially, QSSPC lifetime measurements were performed at one fixed point (10 mm from the bottom of the block) with different filters to compare the lifetime as a function of injection level for the two filters. During the measurements, the optical constant was set to 0.76 and 0.87 for the RG1000 and the EO1050 respectively, which corresponds to absorption up to a depth of 10 mm in the ingot.

The results are shown in FIG. 5a which clearly shows that the measured lifetimes with the filter with the longer cut-off wavelengths are higher at all injection levels. As expected, due to removing the short wavelengths photons from the flash,

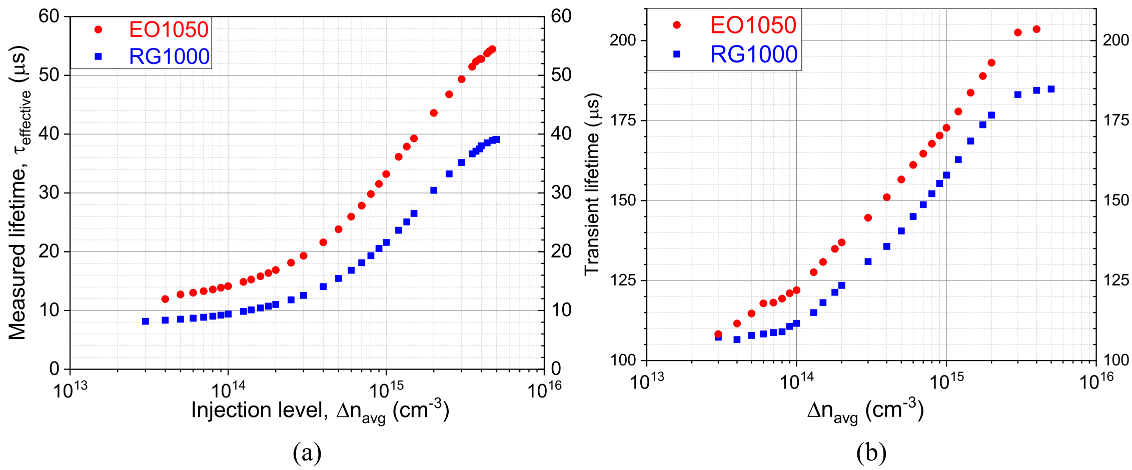


**FIG. 5**. a) Measured QSS lifetimes and b) Transient lifetimes, as a function of injection level for three filters on a standard industrial Cz p-type monocrystalline silicon block. The maximum injection levels are slightly lower when the EO filters are used.

the maximum injection level is slightly lower when the EO1050 filter is used.

We then measured lifetimes in the transient mode, $\tau_{transient}$, at the same point on the block with both filters and compared the reported values with the QSS mode. The transient photoconductance decay method is less prone to the effects of high SRV, and the measured lifetimes are expected to be closer to the actual bulk lifetime. The transient measurement results are presented in FIG. 5b for which the EO filters still have a better performance. The transient lifetimes are in 160-170 μs ranges whereas the QSS effective lifetimes varied from 20 to 35 μs at $\Delta n_{avg}$ = $10^{15}$ $cm^{-3}$.

Due to such a large discrepancy, and the fact that the measured effective lifetime is significantly lower than the actual bulk lifetime, a transfer function is required to remove the effect of high SRV. As illustrated in FIG. 3, the function should transfer $\tau_{effective}$ value to a QSS-bulk lifetime ($\tau_{QSS\text{-}bulk}$) which should ideally be equal to the actual bulk lifetime, $\tau_{bulk}$.

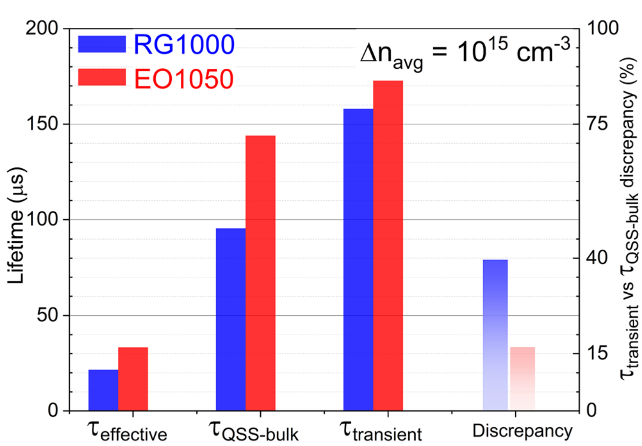


**FIG. 6**. The effective, QSS-bulk, transient lifetimes and discrepancy for different filters at $\Delta n_{avg}$ = $10^{15}$ $cm^{-3}$.

FIG. 6 shows the effective, QSS-bulk, transient lifetimes for both filters at $\Delta n_{avg}$ = $10^{15}$ $cm^{-3}$. The figure also represents a discrepancy percentage for each filter which represents the difference between the $\tau_{QSS\text{-}bulk}$ and the $\tau_{transient}$ for each filter. The current standard RG1000 filter leads to a discrepancy with $\tau_{transient}$ of around 40%. In contrast, the EO1050 performed significantly better, resulting in a $\tau_{QSS\text{-}bulk}$ within 15% of the $\tau_{transient}$. Therefore, due to the lower effects from the transfer function (in comparison with RG1000) as well as the less discrepancy with $\tau_{transient}$, selecting the EO1050 will improve photoconductance lifetime measurements in QSS mode.

## IV. CONCLUSION

This paper demonstrates improved QSSPC effective lifetime measurements, particularly in the lifetime range above 50 μs, on silicon blocks by using deeper photo-generation profiles via filters with longer cut-off wavelengths. Due to the reduced impact of surface recombination in this lifetime range, there is less reliance on the transfer function to estimate the bulk lifetimes in comparison with the standard filter. However, there is a corresponding increase in the uncertainty of the optical factor as the photogeneration becomes deeper, due to the reference cell EQE in the longer-range wavelengths. In addition, carrier generation beyond the coil sensitivity depth counteracts the benefits of reduced surface recombination, which makes the EO1100 filter an unsuitable option for QSS measurements. The comparison between the results from the QSSPC method and transient photoconductance decay method, revealed a reasonable agreement between the results using the EO1050 filter, reducing the discrepancy to around 15%. We conclude that the use of the EO1050 filter is a suitable choice to reduce the uncertainty of the estimated bulk lifetime, due to a decreased reliance on the transfer function, while still allowing a sufficiently accurate estimation of the optical constant.

## ACKNOWLEDGMENTS

This work has been supported by the Australian Renewable Energy Agency (ARENA) through grants RND009 and RND017.

## REFERENCES

[1] R. A. Sinton and A. Cuevas, "Contactless determination of current–voltage characteristics and minority-carrier lifetimes in semiconductors from quasi-steady-state photoconductance data," Applied Physics Letters **69**(17), 2510 (1996).

[2] M. Goodarzi *et al.*, "Accuracy of interstitial iron measurements on P-type multicrystalline silicon blocks by quasi-steady-state photoconductance," IEEE Journal of Photovoltaics **7**(5), 1216–1223 (2017).

[3] J. S. Swirhun, R. A. Sinton, M. K. Forsyth, and T. Mankad, "Contactless measurement of minority carrier lifetime in silicon ingots and bricks," Progress in Photovoltaics: Research and Applications **19**(3), 313–319 (2011).

[4] S. Bowden and R. A. Sinton, "Determining lifetime in silicon blocks and wafers with accurate expressions for carrier density," Journal of Applied Physics **102**(12), 124501 (2007).

[5] S. Johnston, F. Yan, K. Zaunbrecher, M. Al-Jassim, O. Sidelkheir, and K. Ounadjela, "Quality characterization of silicon bricks using photoluminescence imaging and photoconductive decay," in *2012 38th IEEE Photovoltaic Specialists Conference*, 2012, 000406–000410 IEEE.

[6] R. Sinton, T. Mankad, S. Bowden, and N. Enjalbert, "Evaluating silicon blocks and ingots with quasi-steady-state lifetime measurements," in *Proceedings of the 19th European Photovoltaic Solar Energy Conference*, Paris, France, 2004, 520–523.

[7] F. Schindler *et al.*, "Material limits of multicrystalline silicon from state-of-the-art photoluminescence imaging techniques," *Progress in Photovoltaics: Research and Applications* (2016).

[8] B. Mitchell, T. Trupke, J. W. Weber, and J. Nyhus, "Bulk minority carrier lifetimes and doping of silicon bricks from photoluminescence intensity ratios," Journal of Applied Physics **109**(8), 083111 (2011).

[9] J. A. Giesecke, R. A. Sinton, M. C. Schubert, S. Riepe, and W. Warta, "Determination of bulk lifetime and surface recombination velocity of silicon ingots from dynamic photoluminescence," IEEE Journal of Photovoltaics **3**(4), 1311–1318 (2013).

[10] S. Herlufsen, K. Bothe, J. Schmidt, R. Brendel, and S. Siegmund, "Dynamic photoluminescence lifetime imaging of multicrystalline silicon bricks," Solar Energy Materials and Solar Cells **106**, 42–46 (2012).

[11] J. A. Giesecke, M. C. Schubert, F. Schindler, and W. Warta, "Harmonically modulated luminescence: Bridging gaps in carrier lifetime metrology across the PV processing chain," IEEE Journal of Photovoltaics **5**(1), 313–319 (2015).

[12] M. J. Kerr and A. Cuevas, "General parameterization of Auger recombination in crystalline silicon," Journal of Applied Physics **91**(4), 2473–2480 (2002).

[13] M. Goodarzi, R. A. Sinton, and D. Macdonald, "Improving transient photoconductance lifetime measurements on ingots with deeper photogeneration," in AIP Conference Proceedings **1999**(1), 020008 (2018).

[14] N. Schüler, T. Hahn, K. Dornich, J. R. Niklas, and B. Gründig-Wendrock, "Theoretical and experimental comparison of contactless lifetime measurement methods for thick silicon samples," Solar Energy Materials and Solar Cells **94**(6), 1076–1080 (2010).

[15] B. Mitchell, D. Macdonald, J. Schon, J. W. Weber, H. Wagner, and T. Trupke, "Imaging as-grown interstitial iron concentration on boron-doped silicon bricks via spectral photoluminescence," IEEE Journal of Photovoltaics **4**(5), 1185–1196 (2014).

[16] D. Chung, B. Mitchell, M. K. Juhl, M. Abbott, and T. Trupke, "Lifetime imaging on silicon bricks using the ratio of photoluminescence images with different excitation wavelengths," IEEE Journal of Photovoltaics **1-9** (2018).